

# Spin-1/2 frustrated antiferromagnet on a spatially anisotropic square lattice: contribution of exact diagonalizations.

P. Sindzingre

Laboratoire de Physique Théorique des Liquides-UMR 7600 of CNRS, Université Pierre et Marie Curie, case 121, 4 place Jussieu, 75252 Paris Cedex, France  
E-mail: phsi@lptl.jussieu.fr

(May 22, 2019)

The phase diagram of a spin-1/2  $J - J' - J_2$  model is investigated by means of exact diagonalizations on finite samples. This model is a generalization of the  $J_1 - J_2$  model on the square lattice with two different nearest-neighbor couplings  $J, J'$  and may be also viewed as an array of coupled Heisenberg chains. The results suggest that the resonating valence bond state predicted by Nersesyan and Tsvelik [Phys. Rev. B **67**, 024422 (2003)] for  $J_2 = 0.5J' \ll J$  is realized and extends beyond the limit of small interchain coupling along a curve nearly coincident with the line where the energy per spin is maximum. This line is likely bordered on both side by a columnar dimer long range order. This columnar order could extend for  $J' \rightarrow J$  which correspond to the  $J_1 - J_2$  model.

PACS numbers: 75.10.Jm; 75.50.Ee; 75.40.-s

## I. INTRODUCTION

The interplay between frustration and quantum fluctuations in antiferromagnetic (AF) spin-1/2 systems in two dimensions (D) has attracted much experimental and theoretical attention in past years. In particular, many studies have been devoted to identify the possible phases which may appear at  $T = 0$  after the destabilization of a collinear AF Néel phase by quantum fluctuations when increasing frustration in  $SU(2)$  invariant spin models. Large- $N$  approaches predict then a valence bond crystal (VBC) phase, with long range order (LRO) of singlet entities (dimers, plaquettes of resonating dimers...) and thus breaking translational symmetry and/or others space symmetries, if the transition out of the Néel phase is continuous [1–3]. Numerical results obtained from exact diagonalization (ED) studies support this prediction for several models: the  $J_1 - J_2 - J_3$  model on the honeycomb lattice [4] and some models where the spins sit on a square lattice such as the crossed chain model [5,6] and the quadrumerized Shastry-Sutherland model [7].

Yet, for the much studied  $J_1 - J_2$  model on the square lattice, with a next-nearest-neighbor frustrating coupling  $J_2$  in addition to the nearest-neighbor coupling  $J_1$  (see Fig. 1 where the  $J_1 - J_2$  model corresponds to  $J' = J = J_1$ ), the validity of this scenario remain unclear [8–17]. Its classical ground-state has  $(\pi, \pi)$  Néel LRO for  $J_2 < 0.5J_1$  and is the degenerate manifold corresponding to two decoupled Néel states on interpenetrating square

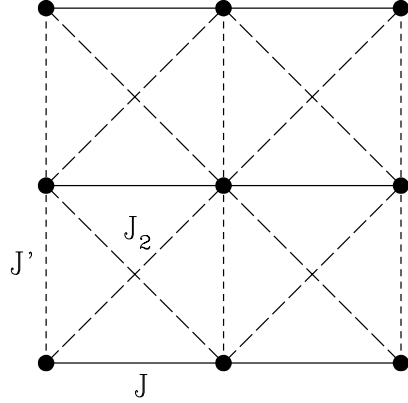


FIG. 1. Exchange interaction pattern in the  $J - J' - J_2$  model. The spins sit at the vertices shown by bullets, the coupling constant is  $J$  between nearest-neighbor pairs on horizontal bonds (full lines),  $J'$  on vertical bonds (short dashed lines) and  $J_2$  on the diagonal bonds (long dashed lines). The  $J_1 - J_2$  model corresponds to  $J' = J = J_1$ .

lattices for  $J_2 > 0.5J_1$ . There is a large consensus that  $(\pi, \pi)$  Néel LRO (see Fig. 2) survives to quantum fluctuations for  $J_2/J_1 \lesssim 0.4$  and these select either a  $(\pi, 0)$  or a  $(0, \pi)$  Néel LRO in the manifold of classical ground-states for  $0.65 \lesssim J_2/J_1$  whereas there is no Néel LRO and a gap to spin excitations in the intermediate range  $0.4 \lesssim J_2/J_1 \lesssim 0.65$ . The transition out of the  $(\pi, \pi)$  Néel phase is second order while the transition out of the  $(\pi, 0)$  Néel phase has been predicted to be of first order [10] but may be close to second order [14].

Whether this intermediate phase has VBC LRO or is some resonating valence bond (RVB) phase which do not break any space symmetries, i.e. a spin-liquid, is debated. Earliest investigations from ED calculations on samples up to  $N = 36$  spins have shown enhanced columnar dimer-dimer correlation in the intermediate region, but the finite-size scaling of the order parameter for the columnar VBC LRO, shown in Fig. 3(a), were not conclusive [8,9]. Dimer series expansions, however, have favored an LRO of columnar dimers [10,11] and latter to two different VBC phases: a columnar dimer phase for  $J_2/J_1 \lesssim 0.5$  and a columnar dimer phase with plaquette

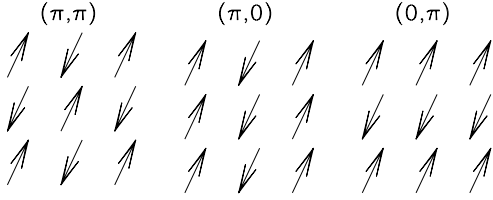


FIG. 2. Spins orders in the classical  $(\pi, \pi)$ ,  $(\pi, 0)$  and  $(0, \pi)$  Néel states

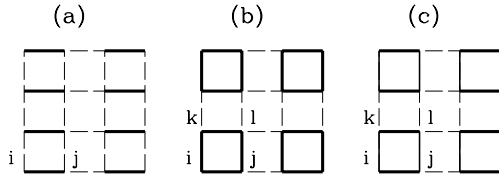


FIG. 3. Patterns of VBC orders proposed for  $J_1 - J_2$  model: (a) columnar dimer, (b) plaquette, (c) columnar dimer with plaquette type modulation. Full lines connect spins bound into singlet: two spins in (a), four spins in (b) and (c). In (b) the strength of spin-spin correlations on vertical and horizontal links of a plaquette  $i, j, k, l$  are the same but differs in (c). There are four degenerate ground-states for orders (a), (b) and eight for the order (c) in the  $J_1 - J_2$  model. These are obtained by one step translations in the horizontal and vertical directions and/or a  $\pi/2$  rotation around a lattice site.

type modulation, as shown in Fig. 3(c), for  $0.5 \lesssim J_2/J_1$ , separated by a second order transition [14]. Studies based on the Green function Monte Carlo method, for systems of sizes larger than those which may be investigated by ED calculations, favored either a plaquette LRO [12], as shown in Fig. 3(b), or a columnar dimer LRO with plaquette type modulation [13], similar to one of Ref [14], for  $J_2/J_1 = 0.5$ . Besides, it was concluded in Ref [12] that the finite size scaling of the susceptibility to columnar dimer LRO from both Monte Carlo and ED calculations would exclude columnar dimer LRO at  $J_2/J_1 = 0.5$ . However, latter calculations [15] by the same group which favored the plaquette LRO [12] have lead to conclude in favor of the occurrence of a spin-liquid phase for  $0.4 \lesssim J_2/J_1 \lesssim 0.5$  whereas it was pointed out that the occurrence of the plaquette LRO will be unlikely in view of the spatial symmetries of the low lying singlets in the ED spectra. In their latest study these authors suggest either a spin-liquid or, possibly, the columnar state but with a weak order parameter [17] Yet, as the Monte Carlo calculations and the series expansions start from some trial state which may bias the results and involve approximations which are not fully under control, while ED calculations which were performed on samples

having different lattice symmetries and display irregular finite size scaling, the nature of the ground-state in the intermediate region remain an open question.

In this paper, motivated by a recent paper of Nersisyan and Tsvelik [18], referred as (NT) in the following, we attempt to shed light on this issue from ED calculations on a spatially anisotropic version of the  $J_1 - J_2$  model with two different nearest neighbor couplings. The Hamiltonian of this  $J - J' - J_2$  model (named the confederate flag model by NT) reads:

$$\mathcal{H} = \sum_m^M \sum_l^L [ J \mathbf{S}_{l,m} \cdot \mathbf{S}_{l+1,m} + J' \mathbf{S}_{l,m} \cdot \mathbf{S}_{l,m+1} + J_2 (\mathbf{S}_{l,m} \cdot \mathbf{S}_{l+1,m+1} + \mathbf{S}_{l,m} \cdot \mathbf{S}_{l+1,m-1}) ] \quad (1.1)$$

which may also be viewed as an array of  $M$  of spin chains of length  $L$ , if  $J' < J$ . The exchange  $J$  (see Fig. 1) couples first-neighbor (horizontal) pairs of spins along the chains,  $J'$  first-neighbor spins in the (vertical) transverse direction and exchange  $J_2$  second-neighbor pairs on the diagonals of the plaquettes. All exchanges are assumed positive, describing AF couplings. For  $J' = J$  one recovers the  $J_1 - J_2$  model. Mostly interested with the limit  $M, L \rightarrow \infty$ , we shall also focus on the case  $J' \leq J$ .

The classical ground-state of the  $J - J' - J_2$  model is rather similar to the one of the  $J_1 - J_2$  model. When  $J' < J$ , one has  $(\pi, \pi)$  Néel LRO if  $J_2 < 0.5J'$ ,  $(\pi, 0)$  Néel LRO if  $J_2 > 0.5J'$  and the  $J$  chains are decoupled if  $J_2 = 0.5J'$  whereas for  $J' > J$ , one has  $(\pi, \pi)$  Néel LRO if  $J_2 < 0.5J$ ,  $(0, \pi)$  Néel LRO if  $J_2 > 0.5J$  and the  $J$  chains are decoupled if  $J_2 = 0.5J$ .

This Hamiltonian has been much studied in past years for a finite number of chains, the so-called  $M$ -leg ladders, generally in the case of open boundary conditions in the transverse direction (for  $M > 2$  since if  $M = 2$  open and periodic boundary conditions are equivalent).

Numerical studies [27–29] based on the density matrix renormalization group (DMRG) method or Monte Carlo approaches have shown that the  $M$ -leg unfrustrated ladders ( $J_2 = 0$ ) display a behavior analogous to a  $M/2$ -spin chain [26], being fully gapped if  $M$  is even and gapless if  $M$  is odd. So  $(\pi, \pi)$  Néel LRO only occurs in the limit  $M \rightarrow \infty$ .

The effect of frustration has been especially investigated theoretically and numerically for the 2-leg ladder (see Ref [21–24] and references therein). These studies have concluded that one has two phases separated by a transition line which has been found to coincide with the line of maximum frustration where the energy per spin reaches its maximum, noted  $J_2^m(J')$  in the following for all values of the number of chains. This line starts as  $J_2^m(J') \sim 0.5J'$  for  $J' \rightarrow 0$  and bend slightly with increasing  $J'$  so that  $J_2^m(J') \sim 0.6$  at  $J' = 1$  [21,22] (as the dashed line in Fig. 4). If  $J_2 > J_2^m(J')$  one has the ‘Haldane phase’, where the two spins on a rung tend to be in a triplet state, so named as it contains the point  $J_2 = J, J' = 0$  whose low-energy spectrum is similar to

that of a spin-1 Heisenberg chain. If  $J_2 < J_2^m(J')$  one has the so called 'singlet phase', so called as it contains the case  $J' \gg J$  with  $J_2 = 0$ , where the ground-state consists of singlets on each rung. As shown by White [32] the 'singlet phase' is also an Haldane phase with diagonally situated next-nearest neighbor spins coupling to form an effective  $S = 1$ . Both phases have a topological order, breaking a hidden  $Z_2 \times Z_2$  symmetry, which can be measured by non-local 'string order' parameters, similar to the string order parameter of the  $S = 1$  Heisenberg chain. The two phases are fully gapped like the  $S = 1$  chain [26], and have a non degenerate singlet ground-state. These ground-states become degenerate on the transition line  $J_2^m(J')$ . The nature of the transition has been debated. In a DMRG study [22] it was predicted that the transition line would be gapless for  $J_2$  lower than  $\approx 0.287J$ . But more recent DMRG calculations [23] have concluded that a gap subsists between the two-fold degenerate ground-state and the excited states for all  $J_2 > 0$ . So the transition is 1th order on the whole line  $J_2^m(J')$  in agreement with bosonization results in the limit of vanishing interchain coupling [24]. The elementary excitations then consist of gapped deconfined spin-1/2 spinons which may be viewed as kinks interpolating between the two ground-states [24]. Note that these results imply that the classical behavior of independent chains on the line  $J_2 = 0.5J'$  is then destabilized by quantum fluctuations. The single Heisenberg chain is gapless. The spectrum of two independent chains too. The existence of a finite gap excludes such a behavior.

A DMRG study of the three-leg frustrated ladder with open boundary conditions in the transverse direction [25] has shown that this system exhibit two phases separated by a transition line also coincident with the line of maximum frustration  $J_2^m(J')$  and which is a curve quasi identical to the one found for the 2-leg ladders. The phases are analogous to those of the 2-leg ladders. The small  $J_2$  phase, which is the phase of the unfrustrated ladder, show a tendency of the three spins on a vertical line to pair in a state of minimum spin whereas they tend to pair in a state of maximum spin in the large  $J_2$  phase, which is equivalent to the spin-3/2 chain. On the transition line a bosonization study at weak interchain coupling [33] has predicted that the ground-state is a chiral spin-liquid.

Recently NT, using an approach based on the bosonization method, investigated the crossover from finite  $M$  to  $M \rightarrow \infty$  in  $J - J' - J_2$  model on the line  $J_2 = 0.5J'$ , in the limit of small interchain coupling ( $J', J_2 \ll J$ ) and predicted that the classical behavior of independent chains is unstable to a special RVB (spin-liquid) state which may be a realization of the chiral  $\pi$ -flux RVB state [18–20]. Its ground-state has a  $2^{M-1}$  degeneracy, for  $M$  even and transverse periodic boundary conditions, associated to the breaking of a local  $Z_2$  symmetry, present in the bosonised version of the model, corresponding to the invariance under independent translations by one lattice spacing along individual chains. Each ground-state may be characterized

by different values of a set of non-local order parameters. These non-local order parameters correlate spins on two adjacent chains whereas different pairs of chains are uncorrelated. The elementary excitations consist of deconfined spin-1/2 spinons interpolating between different ground-states. These excitations are either gapless, as predicted for some values of the number of chains, such as  $M = 4, 6, 12$ , or gapped, as for the 2-leg ladder ( $M = 2$ ).

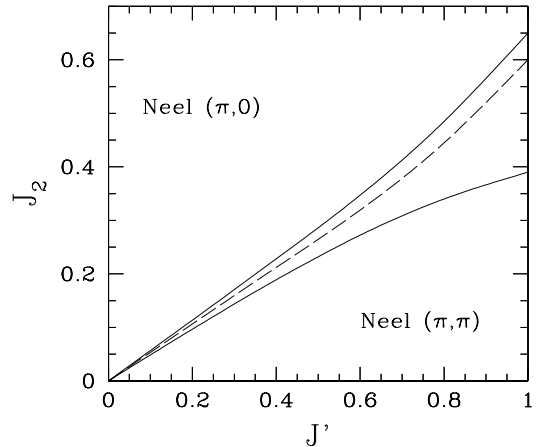


FIG. 4. Proposed phase diagram of the  $J - J' - J_2$  model for  $L \rightarrow \infty$  and  $M \rightarrow \infty$  ( $J = 1$ ). The solid lines indicate the approximate location of the boundaries of the  $(\pi, \pi)$  and  $(\pi, 0)$  Néel phases, noted  $J_2^1(J')$  and  $J_2^2(J')$  respectively. The dashed line in the intermediate region between the Néel phases is the approximate location of the maxima  $J_2^m(J')$  of the energy per spin  $e_0$  along which the present ED results suggest that the RVB state predicted by NT may be realized up to large values of  $J'$ . In the intermediate region, outside the curve  $J_2^m$ , the ground-state is predicted to display columnar dimer order. The Néel phases only appear for both  $L, M \rightarrow \infty$ . For finite  $M$  and  $L \rightarrow \infty$  one has gapped phases. The position of the curve  $J_2^m(J')$  is quasi-independent of the number  $M$  of chains down to  $M = 2$ , which correspond to the 2-leg ladder.

Two questions then arise. First, does the state predicted by NT extends outside the range of small interchain coupling. Second, what is the nature of the behavior in its vicinity, in particular for the case of an infinite number of chains. Below we report results of ED calculations of  $N = M \times L$  spins for  $N \leq 36$  to shed light on these questions and more generally the phase diagram of the  $J - J' - J_2$  model. We shall consider only the case of an even number of chains. The ED calculations have been carried out on samples of  $N = M \times L$  spins in  $M$  chains of lengths  $L$  with periodic boundary conditions both along and perpendicular to the chains: samples of 4 chains with  $N = 16, 24, 32, 36$  spins and 6 chains with  $N = 24, 36$  spins. Additional calculations were also performed for the  $M = 2$  ladder for  $N \leq 32$  in order to

compare with the  $M = 4, 6$  results. Contrary to the samples considered in previous ED calculations for the  $J_1 - J_2$  model, all samples have translation vectors parallel to the basis vectors of the square lattice which leads to a regular evolution of the properties with increasing  $L$  and  $M$ .

Examination of the ED spectra indicates that the model will display two Néel phases, with magnetic wave-vectors  $(\pi, \pi)$  and  $(\pi, 0)$ , separated by a magnetically disordered intermediate region, in the limit  $N \rightarrow \infty$  with both  $L \rightarrow \infty$  and  $M \rightarrow \infty$  as shown in Fig. 4. At variance with a study based on the DRMG method [34], which appeared very recently on a preprint server, our results provide indications that the classical behavior of independent chain is destabilized by quantum fluctuations and the RVB state of NT may occur along a curve coincident with the line of maximum frustration  $J_2^m(J')$ , located in this intermediate region, up to large interchain coupling. They also indicate that the intermediate region of the  $M \rightarrow \infty$  phase diagram (see Fig. 4) on both sides of this line has columnar VBC LRO, which may extend up to  $J' \rightarrow J$  and could already appear for  $M$  even  $\geq 4$ .

In Sec. II we describe the evolution of the energy per spin vs  $J_2$  and  $J'$  and the location of the curve  $J_2^m(J')$ . The properties of the model in the regions of  $(\pi, \pi)$  Néel LRO,  $(\pi, 0)$  Néel LRO and in the intermediate region are described in Sec. III, IV and V, respectively. Conclusions are summarized in Sec. VI.

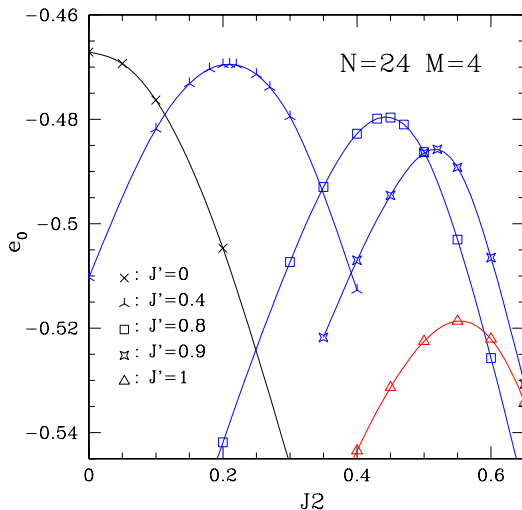


FIG. 5. Ground-state energies per spin  $e_0 = E_0/N$  vs  $J_2$  for the  $N = 24$  sample with  $M = 4$  (4 chains). The lines are guides to the eyes.

## II. ENERGY RESULTS

The ground-state energies per spin  $e_0 = E_0/N$  are plotted, as a function of  $J_2$ , for different values of  $J' \leq 1$

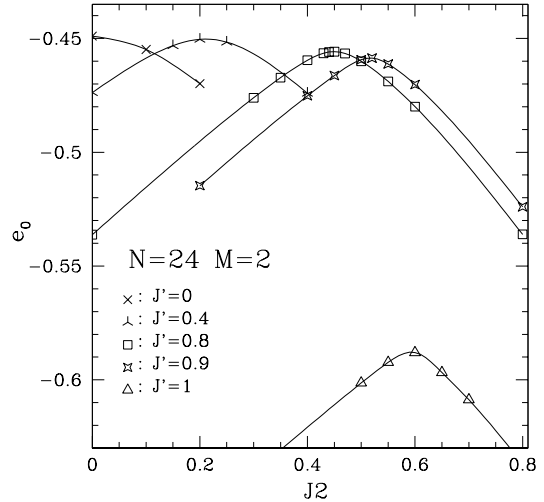


FIG. 6. Same as Fig. 5 for the  $N = 24$  sample with  $M = 2$  (2-leg ladder).

( $J = 1$  in the following) for the  $M = 4$  chains  $N = 24$  sample in Fig. 5. For comparison, the results for the  $N = 24$  2-leg ladders are indicated in Fig. 6. Fig. 7, displays  $e_0$  vs  $J_2$  at  $J' = 0.8$  for the different  $M = 4$  and  $M = 6$  samples. As shown in Fig. 5 and Fig. 7 the point of "maximum frustration" where  $e_0$  reaches its maximum,  $J_2^m(J')$  occurs for a value of  $J_2$  slightly larger than  $0.5J'$ , as found for the two and three-leg ladders [21,22,25].

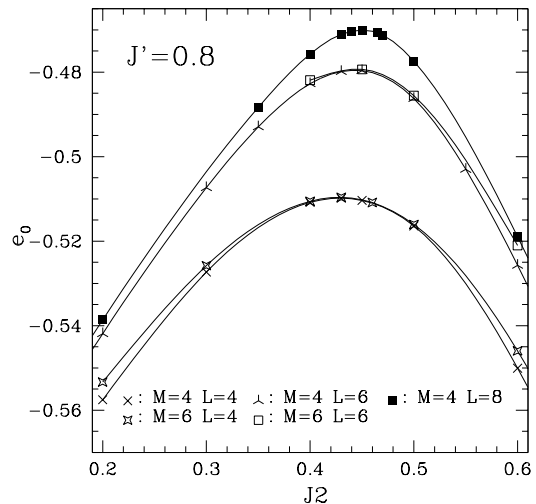


FIG. 7. Ground-state energies per spin  $e_0 = E_0/N$  vs  $J_2$  at  $J' = 0.8$  for different samples of  $M$  chains of lengths  $L$ .

As shown in Fig. 7  $J_2^m$  slightly increases with  $L$  but is nearly independent of the number  $M$  of chains. This indicates that the  $L \rightarrow \infty$  curves  $J_2^m(J')$  will be quasi-

independent of  $M$  as previously conjectured from a comparison of the results for the two and three-leg ladders [25]. The maxima of  $e_0$  (for a given sample) decrease with increasing  $J'$  but remain rather close to the value for decoupled chains at  $J' = 0$  at least if  $J' \leq 0.9$ .

In Fig. 5 and Fig. 6 one sees, in the range  $0.9 < J' < 1$  a drop of  $e_0$  at  $J_2^m$  from a value close to the one for decoupled chains of lengths  $L$  to a value closer to the one for independent chains of lengths  $M$ . This corresponds to the crossover to the situation at  $J' \gtrsim 1$  where the finite samples  $M \times L$  are best viewed as  $L$  coupled chains of finite lengths  $M$ .

### III. $(\pi, \pi)$ NÉEL LONG RANGE ORDER

Increasing  $J_2$  from zero at given  $J' (\leq 1)$ , one finds a range of parameters, which extends to a value we note  $J_2^{c1}(J')$ , slightly smaller than  $0.5J'$  (and thus  $< J_2^m(J')$ ), where the spectra exhibit the features at finite size specific of a system displaying collinear  $(\pi, \pi)$  Néel LRO in the limit  $N \rightarrow \infty$  with both  $L \rightarrow \infty$  and  $M \rightarrow \infty$ . The Néel order breaks  $SU(2)$  and lattice spacial symmetries. Evidence of Néel LRO in the spectra is the presence of lowest eigenlevels in each spin  $S$  sector which form a set of states with energies  $E(S) - E_0 \sim S(S+1)/N$  for  $L \rightarrow \infty$  and  $M \rightarrow \infty$ , the so-called quasi degenerated joint states (QDJS) [35,5] as shown in Fig. 8. These QDJS are well separated, at finite size, from the others lowest excited states (magnons) and collapse on the ground-state faster with  $N$  than the magnons, enabling the breaking of  $SU(2)$  and lattice spacial symmetries. For collinear LRO there is one QDJS for each  $S$  value. The QDJS specific of  $(\pi, \pi)$  Néel LRO consist of a state belonging to an irreducible representation (IR) with wave-vector  $\mathbf{k} = 0$  if  $S$  is even or  $\mathbf{k} = (\pi, \pi)$  if  $S$  is odd, both even in a spatial  $R(\pi)$  rotation around a site and in the reflexion  $\sigma$  with respect to a  $J$  chain.

The approach of ED calculations does not allow an accurate location of boundary of the Néel phase since it is limited to small samples. Nevertheless the extension of the Néel phase can be approximatively estimated from ED calculations by monitoring the range of values of  $J_2$  for which the QDJS remain well defined in the spectrum [5]. This gives  $J_2^{c1}(J' = 1) \approx 0.4$  for the  $J_1 - J_2$  model,  $J_2^{c1}(J' = 0.8) \approx 0.35$ , and shows that  $J_2^{c1}(J')$  moves steadily closer to the line  $J_2 = 0.5J'$  as  $J'$  decreases. Besides, quantum Monte Carlo calculations on the unfrustrated line of the phase diagram ( $J_2 = 0$ ) have indicated that  $(\pi, \pi)$  LRO appear as soon as  $J' > 0$  for  $M \rightarrow \infty$ , which enable to conclude that the Néel LRO extend down to point  $J' = 0, J_2 = 0$  [30].  $J_2^{c1}$  appears to be slightly smaller than  $0.5J'$ , moving away from the line  $0.5J'$  as  $J'$  increases from zero.

It is to be emphasized that Néel LRO appear only for both  $M \rightarrow \infty$  and  $L \rightarrow \infty$ . There is no Néel LRO for a finite number  $M$  of chains. Indeed, as mentioned

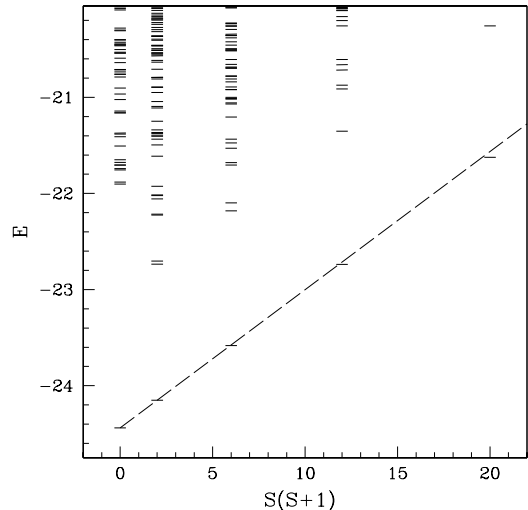


FIG. 8. Spectrum at  $J' = 1$  and  $J_2 = 0$  vs  $S(S+1)$  for  $N = 36$ . The QDJS characteristic of collinear Néel LRO at the bottom of each  $S$  sector are well aligned (dashed line) and clearly separated from the other lowest excitations (see text).

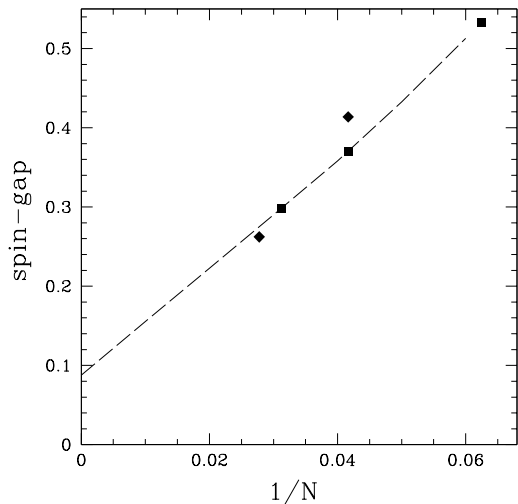


FIG. 9. Spin-gaps at  $J' = 0.8$  and  $J_2 = 0$  vs  $1/N$  for for  $N = 16, 24, 32$  samples of  $M = 4$  chains (squares) and the  $N = 24, 36$  samples of  $M = 6$  chains (diamonds). The dashed line is a spline fit to the  $M = 4$  values for  $N \leq 32$  followed by linear extrapolation for  $N > 32$ .

above, systems which consist of a finite number  $M$  of  $S = 1/2$  Heisenberg chains are known to acquire a gap upon shifting a transverse coupling  $J'$  if  $M$  is even, behaving analogously to a spin  $S = M/2$  chain, so these systems are in a Haldane phase [27–30].

The typical evolution of the spin-gap  $\Delta^1$  with  $M$  and  $L$  is illustrated in Fig. 9 where values of the  $\Delta^1$  are plotted vs  $1/N$  for  $N = 16, 24, 32$  samples of  $M = 4$  chains and the  $N = 24, 36$  samples of  $M = 6$  chains at  $J' = 0.8$  and  $J_2 = 0$ . The evolution for  $M = 4$  of  $\Delta^1$  vs  $1/N \sim 1/L$  shows a small but noticeable upward curvature as found previously for the 2-leg and 4-leg ladders (see Fig.1 of Ref. [27]). So a linear extrapolation beyond  $N > 32$  of a spline fit to the  $M = 4$  three values of  $\Delta^1$  to  $1/L$  (dashed line in Fig. 9) leads to a lower bound of  $\Delta^1$  for  $L \rightarrow \infty \sim 0.09$  which shows that  $\Delta^1(L \rightarrow \infty)$  remains finite. Corrections to this extrapolated value are nonetheless probably non negligible. The true value of  $\Delta^1$  for  $L \rightarrow \infty$  for  $M = 4$  is likely somewhat closer to the value ( $\sim 0.14$ ) estimated for the 4-leg ladder with open boundary conditions in the transverse direction [28]. For  $M = 6$ , the present data, limited to the two values for  $L = 4, 6$ , show that  $\Delta^1(L \rightarrow \infty)$  decreases with increasing  $M$ , and remain finite if  $M = 6$ . Its value for the 6-leg ladder is  $\sim 0.04$  [28] if  $J' = 0.8$ . The present data show that the gap is very small but do not allow an accurate estimation of a gap of this order of magnitude.

The evolution of the spin-gap with  $N \rightarrow \infty$  for  $M = L$  is different than for fixed  $M$  and  $L \rightarrow \infty$ . For  $M = L$ , where  $\Delta^1 \rightarrow 0$  for  $N \rightarrow \infty$ , the  $N = 16, 36$  values in Fig. 9 indicates an evolution of the spin-gap in the case  $M = L$  that decreases with a negative curvature vs  $1/N$  as usually found in systems with Néel LRO [31].

#### IV. $(\pi, 0)$ NÉEL LONG RANGE ORDER

For  $J_2$  larger than a value  $J_2^{c2}$ , larger but very close to  $J_2^m$ , one similarly recognizes in the spectra, the features specific of collinear Néel LRO with a wave vector  $(\pi, 0)$  or  $(0, \pi)$  depending on value of  $J'/J$ .

If  $J' = J = 1$  and  $M = L$  these two Néel orders are degenerate. The QDJS then include two states for each value of  $S$ : two with  $\mathbf{k} = 0$  if  $S$  is even and two with  $\mathbf{k} = (\pi, 0)$  and  $\mathbf{k} = (0, \pi)$  if  $S$  is odd, all even in  $R(\pi)$  and  $\sigma$ .

The degeneracy is lifted if  $J' \neq J$ . For  $J' < J$  and in the thermodynamic limit  $M = L \rightarrow \infty$  the  $(\pi, 0)$  LRO is favored whereas this would be  $(0, \pi)$  LRO for  $J' > J$ . The QDJS of  $(\pi, 0)$  LRO are observed as the lowest states of the spectra as soon as  $J' < J$  for  $M = L$ . They include only one state for each value of  $S$ : a state with  $\mathbf{k} = 0$  if  $S$  is even and a state with  $\mathbf{k} = (\pi, 0)$  if  $S$  is odd, both even in  $R(\pi)$  and  $\sigma$ .

Note, however, that at finite size, for an aspect ratio  $M/L < 1$  of the samples, quantum fluctuations, which favor an antiferromagnetic allignment of the spins in the

shortest direction, lead to spectra characteristic of  $(0, \pi)$  LRO even for  $J' < J$  as  $J' \approx J$ . The transition between the two kind of spectra then occurs in the range of values of  $J'$  where  $e_0$  at  $J_2^m(J')$  drops to a value similar to the one of  $L$  decoupled chains (see Fig. 5). For  $M = 4$  and  $L > M$ , it is only for  $J' \lesssim 0.9$  that the QDJS of  $(\pi, 0)$  LRO becomes lower than the QDJS of  $(0, \pi)$  LRO.

The boundary of the  $(\pi, 0)$  Néel phase can be also estimated in the same way as for the  $(\pi, \pi)$  phase. For the  $J_1 - J_2$  model it was found that  $J_2^{c2}$  occurs at a value slightly larger than  $J_2^m \approx 0.6$ , in the range  $0.60 < J_2^{c2}(J' = 1) < 0.70$ . Examination of the spectra for  $J' < 1$  indicates that  $J_2^{c2}$  move closer to  $J_2^m$  as  $J'$  decreases with  $J_2^{c2} \approx 0.5J'$  for  $J' \rightarrow 0$ . As at  $J_2 = 0$ , for Heisenberg chain coupled by  $J'$  interactions, it is likely that, at  $J' = 0$ , the 1D behavior of the single Heisenberg chain is unstable to  $J_2$  interchain coupling leading to Néel LRO as soon as  $J_2 > 0$ .

Here too, the Néel LRO appears only in the limit of an infinite number of chain. The spin-gap remains finite at  $M$  fixed for  $L \rightarrow \infty$ . The ground-state is a non degenerate singlet. One has Haldane-like phases. Instead of the  $(\pi, \pi)$  Néel LRO one has the same phase as the phase of the  $M$ -leg (unfrustrated) ladder. In place of the  $(\pi, 0)$  Néel LRO one has a phase, that is probably closely similar to the one of the spin- $M/2$  chain as found for the 2-leg and 3-leg ladders. These phases are analogues of the 'singlet' and 'Haldane' phases of 2-leg ladder. Like the 2-leg ladder they have likely an hidden topological LRO. This and their eventual relation to the chain of integer spins  $S > 1$  for which string order parameters have been recently studied [36] deserves further investigation.

#### V. INTERMEDIATE REGION

Between these two regions of Néel behavior, there is a range of parameters  $J_2^{c1}(J') \leq J_2 \leq J_2^{c2}(J')$  where the spectra indicate an absence of Néel LRO when  $L \rightarrow \infty$  and  $M \rightarrow \infty$ . Leaving the region of  $(\pi, \pi)$  Néel LRO by increasing  $J_2$  at constant  $J'$ , the evolution of the energies of the lowest eigenstates in each  $S$  sector changes to  $E(S) - E_0 \sim S$  for small values of  $S$  (see Fig. 10). This feature is an indication that the spin-gap opens for  $L \rightarrow \infty$  and  $M \rightarrow \infty$  [37] and one enters a magnetically disordered region. At the same time one observes a lowering of some singlet states. This linear behavior reaches its maximum extension for a value of  $J_2$  that appears to coincide with  $J_2^m$  where it extends up to  $S = M/2$  if  $J' \lesssim 0.9$  as shown in Fig. 11 for  $M = 4$  at  $J' = 0.8$ . Then, beyond  $J_2^m$ , the evolution of the lowest eigenenergies returns fast to  $E(S) - E_0 \sim S(S + 1)$  in the  $(\pi, 0)$  Néel region which starts close to  $J_2^m$ .

The quantum numbers of the first excitations in each spin sector and the signs of the spin-spin correlations remain the same as in the  $(\pi, \pi)$  Néel region for  $J_2 \lesssim J_2^m$  and are the same as in  $(\pi, 0)$  region for  $J_2 \gtrsim J_2^m$ . The

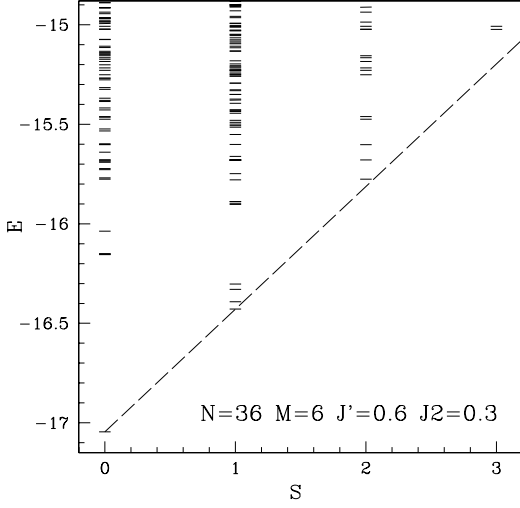


FIG. 10. Spectrum of eigenenergies vs total spin  $S$  for the  $M = 6$  sample of  $N = 36$  spins at  $J' = 0.6$  and  $J_2 = 0.3$ . These values of  $J'$  and  $J_2$  correspond to a point in the intermediate region (slightly) below the line  $J_2^m(J')$  in Fig. 4 ( $J_2^m(J' = 0.6) \approx 0.32$ ). The dashed line, fitted to the lowest  $S = 1$  and  $S = 0$  states, shows that the energy of the lowest states in each spin sector increase nearly as  $\sim S$  at small  $S$  values.

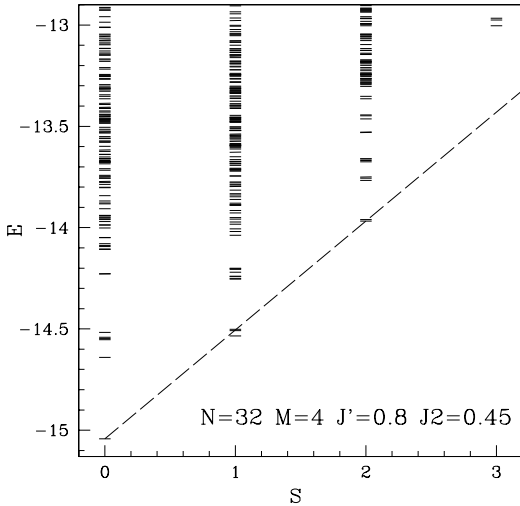


FIG. 11. Spectrum at  $J' = 0.8$  and  $J_2 = 0.45$  for the  $N = 32$  sample of  $M = 4$  chains

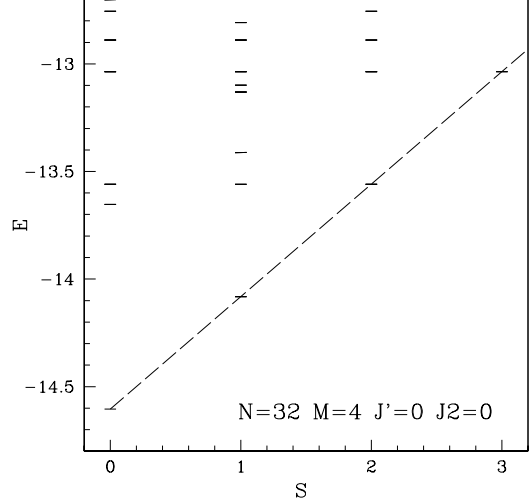


FIG. 12. Spectrum of decoupled chains for the  $N = 32$  sample of  $M = 4$  chains ( $J' = 0$  and  $J_2 = 0$ ). Note that the excited levels have a large degeneracy.

curve  $J_2^m(J')$  is the analogue of the transition line of the classical model  $J_2 = 0.5J'$ . On this line the classical ground-state consist of decoupled chains. Then for  $J_2 \approx J_2^m(J')$  one may notice features, in the spectra and the spin-spin correlations (observed for  $M = 2, 4, 6$ ), that present certain similarities with those of  $M$  decoupled chains if  $J' \lesssim 0.9$  (and those of  $L$  independent chains when  $L > M$  and  $J' \gtrsim 0.9$ ).

As indicated above, one has  $E(S) - E_0 \sim S$  up to  $S = M/2$  as for decoupled chains (see Fig. 12) which is what would result for independent magnetic excitations on the chains. Moreover the very lowest eigenstates in each  $S$  sector belong to the same IR as those of a system of decoupled chains. For instance, the first triplets excitations is a set of  $M$  states with all wave-vectors of type  $(\pi, k_y)$  on the side the Brillouin zone which become quasi degenerate at  $J_2 \approx J_2^m$  as shown in Fig. 13 for the  $M = 4$ ,  $N = 24$  sample at  $J' = 0.8$ . Similarly first excitations at  $S \geq 1$  and  $S \leq M/2$  have same quantum numbers (wave vector, characters in point-group symmetries) as those of decoupled chains which result from the combination of first triplets excitations. The energies per spin (see Fig. 7) and the spin gaps at finite size are also quasi independent of the number of chains.

In addition the spin excitations appear quasi gapless. Although the finite-size spin-gaps are maximum for  $J_2 \approx J_2^m$  as shown in Fig. 13, the analysis of the evolution of the spin-gap  $\Delta^1$  of the  $M = 4$  samples with  $1/L$  indicates that its value at  $L \rightarrow \infty$  is minimum for  $J_2 \approx J_2^m$  as for the 2-leg ladder [22,23]. If  $J' \leq 0.6$  the scaling behavior of  $\Delta^1$  is similar to the one for the single chain (its evolution with  $1/L$  is quasi linear with a very small *negative* curvature) and the  $\Delta^1$  extrapolates to  $\approx 0$ . At  $J' \gtrsim 0.8$  nevertheless the evolution of  $\Delta^1$  with

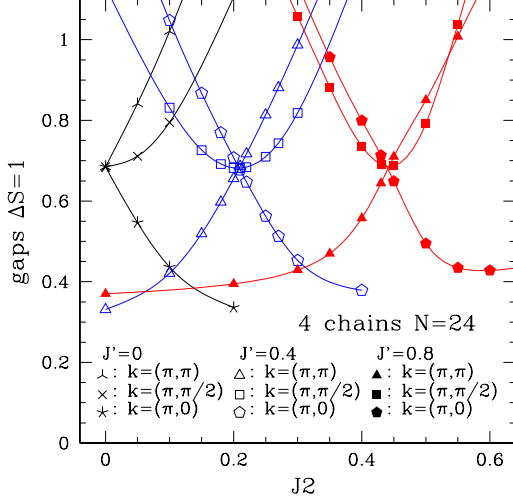


FIG. 13. Gaps to the 1th triplet ( $\Delta S = 1$ ) vs  $J_2$  for  $N = 24$  samples with  $M = 4$  (4 chains) and wave vectors  $k = (\pi, k_y)$  on the side of the Brillouin zone if  $J' = 0, 0.4, 0.8$ . The lines are guides for the eye.

$1/L$  turns to have a positive curvature and  $\Delta^1$  extrapolates to a finite (but small) value. This may be consistent with a spin-gap opening exponentially with increasing  $J'$  along  $J_2^m(J')$  as predicted by NT at weak interchain coupling along  $J_2 = 0.5J'$ . However the spin-gap appears to remain very small up to large interchain coupling.

An apparent decoupling of the chains is also manifest in the spin-spin correlation between two spins at distance  $(l, m)$ :

$$s(l, m) = \langle \mathbf{S}_{0,0} \cdot \mathbf{S}_{l,m} \rangle. \quad (5.1)$$

Values of  $s(l, m)$  for the  $N = 32$  ( $M=4$ ) sample are displayed vs  $J_2$  at  $J' = 0.8$  in Fig. 14 for pair of spins on the same ( $m = 0$ ) or different ( $m = 1, 2$ ) chains at short distances along the chains ( $l \leq 2$ ). Since  $s(l, m)$  decrease in magnitude at given  $m$  with increasing distance  $l$  along the chains these are the largest values of  $s(l, m)$ .  $J_2^m \approx 0.45$  when  $J' = 0.8$  and  $N = 32$ . As shown in Fig. 14 the inter-chain spin-spin correlations become very small at  $J_2 = 0.45$ : if  $m \neq 0$ ,  $s(l, m) \approx 0$  except between first neighbor spins which changes of sign at a slightly larger  $J_2$  value.

Others features in the spectra nevertheless testify of interactions between the chains when  $J_2 \approx J_2^m(J')$ . Starting from situation of decoupled chains at  $J' = 0$  and increasing  $J'$  along  $J_2^m(J')$  one sees a modification of the structure of the eigenlevels above the most lowest eigenstates in each  $S$  sector. Levels which were degenerate for uncoupled chains move away from one-another. In particular, there is a large number of singlet states which separate from the others and drift toward the ground state (from an energy  $\approx$  twice the spin-gap at  $J' = 0$  to an energy  $\sim$  to the spin-gap at  $J' = 0.8$  as shown in

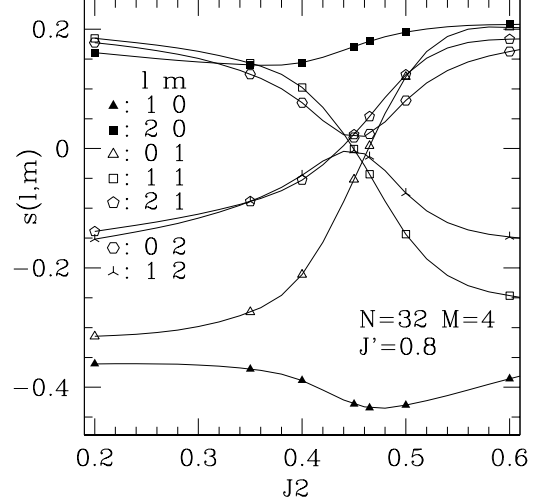


FIG. 14. Spin-spin correlations  $s(l, m)$  (Eq 5.1) between spins at distance  $(l, m)$  vs  $J_2$  for  $N = 32$ ,  $M = 4$ ,  $J' = 0.80$ . The lines are guides for the eye.

Fig. 11 for the  $N = 32$  ( $M = 4 \times L = 8$ ) sample). This could indicate a behavior at  $J_2 \approx J_2^m$  that differs from the one of independent chains and raises the question whether it corresponds to the RVB state predicted by NT in the limit of small interchain coupling for  $J_2 = 0.5J'$ .

We investigate below successively the three cases  $J_2 < J_2^m$ ,  $J_2 \approx J_2^m$  and  $J_2 > J_2^m$  in more detail. In order to be with an intermediate region sufficiently wide and to observe effects of interactions between the chains on small samples we shall mainly display results for a rather large  $J' = 0.8$  value and discuss their evolution for smaller and larger values of  $J'$ .

### A. $J_2 < J_2^m$

For  $J_2 < J_2^m$  and not too close to  $J_2^m$ , the lowest excited singlet states, noted below  $|1\rangle$ ,  $|2\rangle$ ,  $|3\rangle$  are:  $|1\rangle$  in the trivial IR (quantum numbers:  $\mathbf{k} = 0, R(\pi) = 1, \sigma = 1$ ),  $|2\rangle$  [ $\mathbf{k} = (\pi, 0), R(\pi) = -1, \sigma = 1$ ] and  $|3\rangle$  [ $\mathbf{k} = (0, \pi), R(\pi) = -1, \sigma = -1$ ].

Fig. 15 shows the evolution of the singlet-gaps  $\Delta_i^0$  from the ground-state  $|0\rangle$  to the states  $|i\rangle$  vs  $1/L$  at  $J' = 0.8$  and  $J_2 = 0.4$  for the  $M = 4, N = 16, 24, 32$  samples. The gaps evolve with an upward curvature. Linear extrapolations of the gaps for  $N > 32$  give positive values for  $\Delta_1^0, \Delta_3^0$  and a negative value for  $\Delta_2^0$ . This indicates finite gaps  $\Delta_1^0, \Delta_3^0$  and a possible vanishing of  $\Delta_2^0$  for  $L \rightarrow \infty$ . A similar analysis of the values of the  $M = 6, N = 24, 36$  samples also point to the same conclusions for  $L \rightarrow \infty$  if  $M = 6$ .

Yet, the vanishing of  $\Delta_2^0(L \rightarrow \infty)$  for  $M \leq 4$  may be questioned since the 2-leg ladder ( $M = 2$ ) is known to be fully gapped if  $J_2 \neq J_2^m$  [23]. The same analysis indeed

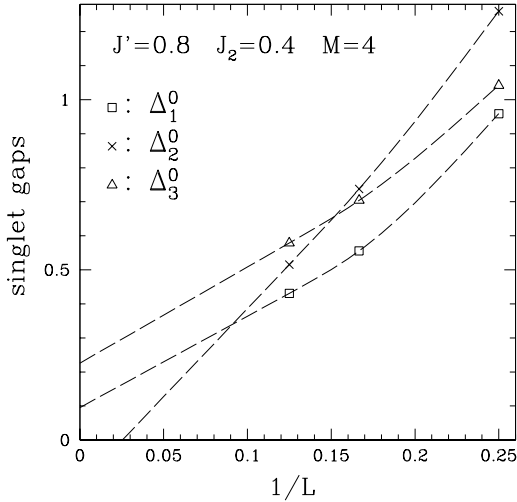


FIG. 15. Singlet-gaps  $\Delta_i^0$  at  $J' = 0.8$  and  $J_2 = 0.4$  vs  $1/L$  for for  $N = 16, 24, 32$  samples of  $M = 4$  chains. The dashed lines are spline fits to the data for  $N \leq 32$  followed by linear extrapolation for  $N > 32$ .

shows that  $\Delta_2^0(L \rightarrow \infty)$  is finite and rather large if  $M = 2$  at  $J' = 0.8$  and  $J_2 = 0.4$ . From this, it could be argued that  $\Delta_2^0(L \rightarrow \infty)$  decreases with  $M$  but remains finite for  $M$  finite. Our data, limited to small sizes cannot exclude this possibility. However  $\Delta_2^0$  most likely vanish on  $J_2^m$  for  $M \leq 4$  (see Sec. V B) while the range of values of  $J_2$  where  $\Delta_2^0$  appear to vanish starts at  $J_2 \approx 0.35$  and extends beyond  $J_2^m$  till  $J_2 \approx 0.5$  (see below) if  $M = 4$ . This range is large which support a vanishing of  $\Delta_2^0$  on an extended range of values of  $J_2$ . An other possibility, is that the value of  $J_2$  at given  $J'$  beyond which  $\Delta_2^0(L \rightarrow \infty)$  would vanish vary with  $M$  and drift toward  $J_2^m$  as  $M$  decreases. ED calculations indeed point out that  $\Delta_2^0(L \rightarrow \infty)$  drops to a minimum at  $J_2 \approx J_2^m$  for  $M = 2$  where this gap is quasi-vanishing.

On the other hand, an analysis of the evolution of the spin-gap  $\Delta^1$  with  $1/L$  show that it remain finite if  $L \rightarrow \infty$  for  $M = 4$  and  $J_2 \leq J_2^m$ . Besides the fact that  $E(S)$  neither evolve as  $E(S) - E_0 \sim S(S+1)$  or as  $E(S) - E_0 \sim S$  indicate that the spin-gap is finite for  $L \rightarrow \infty$  and  $M \rightarrow \infty$ .

All together, the ED results suggest the occurrence of a  $(\pi, 0)$  VBC LRO at  $J' = 0.8$  for  $J_2 \gtrsim 0.35$ , breaking translational symmetry in the horizontal direction with a twice degenerate ground-state, gapped to others singlet and magnetic excitations, possibly as soon as  $M = 4$  when  $M$  is even, and most likely when  $M \rightarrow \infty$ .

The patterns of dimer-dimer correlations

$$D(i, j; k, l) = \langle (\mathbf{S}_i \cdot \mathbf{S}_j)(\mathbf{S}_k \cdot \mathbf{S}_l) \rangle - \langle \mathbf{S}_i \cdot \mathbf{S}_j \rangle \langle \mathbf{S}_k \cdot \mathbf{S}_l \rangle \quad (5.2)$$

between valence bonds on pairs sites  $(i, j)$  and  $(k, l)$  are displayed in Fig. 16 for the  $N = 32$  sample at  $J' = 0.8$

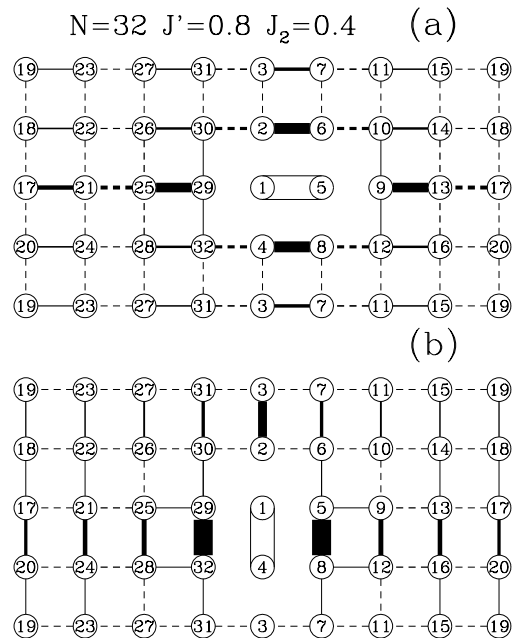


FIG. 16. Dimer-dimer correlation function  $D(i, j; k, l)$  (Eq 5.2) of a dimer on a reference pair of sites  $(i, j)$  with a dimer on a pair of sites  $(k, l)$  for  $N = 32$ ,  $J' = 0.80$ ,  $J_2 = 0.4$ . The reference bond:  $(1, 5)$  in (a),  $(1, 4)$  in (b), is represented by a double line. A solid (dashed) line means a positive (negative) value of  $D$ . The thickness of the line is proportional to the magnitude of  $D$ .

and  $J_2 = 0.4$ . Fig. 16(a) is consistent with a columnar  $(\pi, 0)$  VBC LRO although the correlations between horizontal dimers on different chains are rather small. Fig. 16(b) shows nonetheless correlations between vertical dimers that are not smaller than those between horizontal dimers and that could be consistent with a columnar  $(0, \pi)$  VBC LRO. This may be related to the fact that  $\Delta_2^0$  at  $L = 8$  is still higher than the singlet gaps  $\Delta_1^0, \Delta_3^0$ . It is the extrapolation of  $\Delta_1^0, \Delta_3^0$  at  $L \rightarrow \infty$  to finite values that exclude a  $(0, \pi)$  VBC LRO for  $J' = 0.8$ . In Fig. 16 we see that the dimer correlations are strongest between pair of bonds on adjacent chains and much weaker otherwise. These features reinforce with increasing  $J_2$  and will be maximum at  $J_2 \approx J_2^m$ . Simultaneously, the extrapolated values of  $\Delta_1^0, \Delta_3^0$  at  $L \rightarrow \infty$  decrease toward zero. If  $J' \lesssim 0.9$ , the same features for the singlet gaps and the dimer correlations remain in the intermediate region for  $J_2 < J_2^m$ .

Interchanging the role of  $J$  and  $J'$  in the preceding analysis points out that a  $(0, \pi)$  VBC could occur for finite  $L$  if  $M \rightarrow \infty$  at sufficiently large  $J'$ . On the other hand, VBC LRO for finite  $M$ , in the limit  $L \rightarrow \infty$ , may be excluded at large  $J'$ . As mentioned in Sec. II, there is a crossover in the range  $0.9 < J' < 1$  to a situation where the systems, for an aspect ratio  $M/L < 1$ , may be best viewed as an array of  $L$  chains in the vertical directions. For larger  $J'$  the evolutions of the above singlet gaps with  $1/L$  show that  $\Delta_2^0$  opens and all gaps are finite at  $L \rightarrow \infty$  for  $M = 4, 6$ . The  $(\pi, 0)$  VBC LRO then disappear. In particular, there is no VBC LRO for  $M$  finite if  $J' = J = 1$ . The gaps nevertheless decrease at fixed  $L$  for

increasing  $M$  and the value of  $J'$  where the crossover occurs for  $M/L < 1$  shifts with increasing values of  $M$  to  $J' = J$  for  $M/L \rightarrow 1$ . Thus  $(\pi, 0)$  VBC LRO may extend to  $J' \rightarrow J$  if  $L, M \rightarrow \infty$  where it would be degenerate with  $(0, \pi)$  VBC LRO.

However an analysis of the evolution of the gaps  $\Delta_1^0$ ,  $\Delta_2^0$ ,  $\Delta_3^0$  with the size of the samples one may study by the ED method do not allow to conclude that these gaps vanish at  $J' = J = 1$  for  $N \rightarrow \infty$ , as required for the four-fold degenerate columnar order corresponding to degenerate  $(\pi, 0)$  and  $(0, \pi)$  orders.

It could be possible that one has  $(\pi, 0)$  LRO for  $J' < 1$  and  $(0, \pi)$  LRO for  $J' > 1$  but that VBC LRO vanishes on the line  $J' = J$ . However, the transition out of  $(\pi, 0)$  VBC phase might be first order: the gap  $\Delta_2^0$  appear to jump to a large value going through the transition by increasing  $J'$ . The order parameter would then be finite on the transition line and if this transition line extends to the line  $J' = J$  for  $L = M \rightarrow \infty$ , it would imply that the four-fold columnar order occurs on the line  $J' = J$  where the  $J - J' - J_2$  model reduces to the  $J_1 - J_2$  model. A picture of the dimer correlations similar to the one observed above for at  $J' = 0.8$  and  $J_2 = 0.4$  with strongly correlated pair of chains has been found in dimer series expansions approaches for the  $J_1 - J_2$  model when  $0.4 \lesssim J_2 \lesssim 0.5$  [10]. The pattern of dimer correlations in one of the four-fold degenerate columnar states would then be reminiscent of the one off the line  $J' = J$ .

The locations of the end of the  $(\pi, \pi)$  Néel phase (for  $M \rightarrow \infty$ ) and of the beginning of the  $(\pi, 0)$  VBC phase may differs [16]. They are difficult to estimate accurately from ED calculations with the present sizes but are probably very close or coincident as conjectured for the  $J_1 - J_2$  model [16].

### B. $J_2 \approx J_2^m$

$J_2^m$  is  $\approx 0.45$  at  $J' = 0.8$ . At  $J' = 0.8$  and  $J_2 = 0.45$ , the evolution of the gaps to the first triplet for  $M = 4$  with  $1/L$  (not shown) indicates that the spin-gap remains finite  $L \rightarrow \infty$  although it has become much smaller than at  $J_2 < J_2^m$ . The new feature is the appearance of other singlet states in the low part of the spectrum which, at first sight, appear to form a set of states separated from the singlet continuum (see Fig. 11). This set includes the lowest states with wave vector  $\mathbf{k} = (0, k_y)$  [ $k_y = 2\pi m/M$   $m \in [M/2 - 1, \dots, M/2]$ ] even under  $\sigma$ : the two states noted  $|4 \rangle$  [ $\mathbf{k} = (0, \pm\pi/2)$ ,  $\sigma = 1$ ] if  $M = 4$  or the states [ $\mathbf{k} = (0, \pm\pi/3)$ ,  $\sigma = 1$ ], [ $\mathbf{k} = (0, \pm 2\pi/3)$ ,  $\sigma = 1$ ] if  $M = 6$ , then noted  $|4 \rangle$  and  $|4' \rangle$ . If  $M = 4$ , there also the 2th excited state in the trivial IR, noted  $|5 \rangle$ , just above the states  $|1 \rangle$ ,  $|2 \rangle$ ,  $|3 \rangle$ ,  $|4 \rangle$  whereas if  $M = 6$ , there are also the lowest states [ $\mathbf{k} = (\pi, \pm\pi/3)$ ,  $\sigma = -1$ ], then noted  $|6 \rangle$ . Next if  $M = 4$ , one has just below the singlet continuum a state, noted  $|6 \rangle$ , with [ $\mathbf{k} = (\pi, \pm\pi/2)$ ,  $\sigma = -1$ ], whereas if  $M = 6$ , one finds,

adjacent to the singlet continuum the 2th excited state in the trivial IR (noted  $|5 \rangle$ ) followed by states with wave vectors  $\mathbf{k} = (0, k_y)$ .

This low energy spectrum is different from the one for independent chains to which it may be compared. In the case of decoupled chains the lowest singlets above the ground-state (see Fig. 12) is the degenerate set  $\mathcal{S}_1$  of  $M$  states with wave vectors  $\mathbf{k} = (\pi, k_y)$  ( $k_y = 2\pi m/M$   $m \in [M/2 - 1, \dots, M/2]$ ) which consists of  $|2 \rangle$ ,  $|6 \rangle$  and the state [ $\mathbf{k} = (\pi, \pi)$ ,  $R(\pi) = -1$ ,  $\sigma = 1$ ], noted  $|8 \rangle$  if  $M = 4$  whereas it includes  $|2 \rangle$ ,  $|6 \rangle$ ,  $|8 \rangle$  and the state [ $\mathbf{k} = (\pi, \pm 2\pi/3)$ ,  $\sigma = -1$ ] noted  $|8' \rangle$  if  $M = 6$ . These states correspond to  $S = 0$  lowest excitations along individual chains (which wave vector differs from the one of the ground-state by  $\Delta k = \pi$ ). Just above this set, one has the set  $\mathcal{S}_2$  of  $C_M^2$  degenerate states with wave vector  $\mathbf{k} = (0, k_y)$  which consists of  $|1 \rangle$ ,  $|3 \rangle$ ,  $|4 \rangle$ ,  $|5 \rangle$  and the state [ $\mathbf{k} = (0, \pi)$ ,  $R(\pi) = 1$ ,  $\sigma = 1$ ], noted  $|7 \rangle$  if  $M = 4$  (6 states), whereas if  $M = 6$ , it includes  $|1 \rangle$ ,  $|3 \rangle$ ,  $|4 \rangle$ ,  $|4' \rangle$ ,  $|5 \rangle$ ,  $|8 \rangle$ , a 3th state in the trivial IR, a second state in the same IR as  $|4 \rangle$  and two states in the same IR as  $|4' \rangle$  (15 states). These states correspond to the combination of two  $S = 1$  lowest excitations on different chains in a total singlet state (the lowest  $S = 1$  excitations of the single chain has a wave vector which differs from the one of the ground-state by  $\Delta k = \pi$ ). Third, one has a set  $\mathcal{S}_3$  of  $M$  states with wave vectors  $\mathbf{k} = (\pi, k_y)$ . These states are: [ $\mathbf{k} = (\pi, 0)$ ,  $R(\pi) = -1$ ,  $\sigma = -1$ ], [ $\mathbf{k} = (\pi, \pi/2)$ ,  $\sigma = 1$ ], [ $\mathbf{k} = (\pi, \pi)$ ,  $R(\pi) = -1$ ,  $\sigma = -1$ ] if  $M = 4$ . They correspond to the combination of three lowest  $S = 1$  excitations on different chains. Above  $\mathcal{S}_3$  appear sets of states with wave vectors inside the Brillouin zone which involve higher excitations on individual chains at  $\Delta k \neq \pi$  and appear to form a continuum. At small values of  $L$ ,  $\mathcal{S}_1$ ,  $\mathcal{S}_2$  remain well separated from this continuum which starts at  $\mathcal{S}_3$ . Yet, in the limit  $L \rightarrow \infty$  the gaps to the states of  $\mathcal{S}_1$ ,  $\mathcal{S}_2$ ,  $\mathcal{S}_3$ , vanishes as the gaps to the lowest  $S = 0, 1$  excited states of a single chain. The excited states form a gapless continuum adjacent to the ground-state.

On the line of maximum frustration, the degeneracy in the sets  $\mathcal{S}_1$  and  $\mathcal{S}_2$  appears to be lifted by interchain couplings. Fig. 17 shows the variation of the gaps  $\Delta_i^0$  for the  $N = 32$  sample vs  $J'$  for values of  $J_2 \approx J_2^m(J')$ . The three states  $|2 \rangle$ ,  $|6 \rangle$ ,  $|8 \rangle$  of  $\mathcal{S}_1$  splits. The gaps  $\Delta_2^0$ ,  $\Delta_6^0$  decrease with increasing  $J'$ , while  $\Delta_8^0$  increases. The set  $\mathcal{S}_2$  separate in two groups. The first group consists of the states  $|1 \rangle$ ,  $|3 \rangle$ ,  $|4 \rangle$  which remain very close in energy up to  $J' = 0.6$ . Their gaps decrease with increasing  $J'$ . The second group includes the states  $|5 \rangle$ ,  $|7 \rangle$  which remain at approximatively the same energy up to  $J' \sim 0.6$ . Beyond this value,  $|5 \rangle$  decreases rather abruptly to an energy close to the first group, a drop which may be attributed to the proximity of the range of values of  $0.9 < J' < 1$  where the crossover to the large  $J'$  behavior occurs (for  $J' = 0.9$  additional singlet states which evolve from the lowest singlet states of  $L$  independent chains will begin to appear in the low part the spectrum if  $N =$

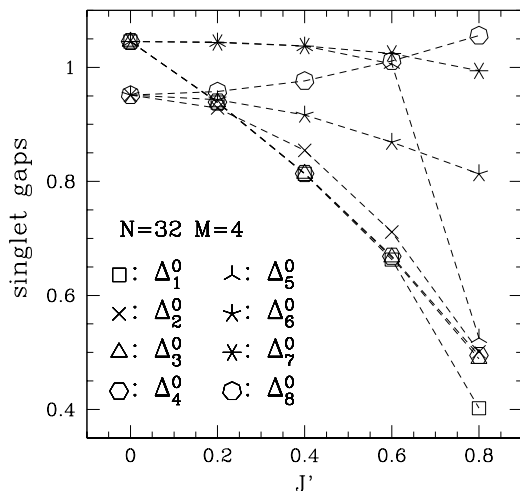


FIG. 17. Singlet-gaps  $\Delta_i^0$  (see text) of the  $N = 32$   $M = 4$  sample vs  $J'$  for values of  $J_2 \approx J_2^m(J')$ . The dashed lines are guide to the eyes.

32). A similar splitting also occurs in most of the sets of states which are above  $\mathcal{S}_3$  (the states of  $\mathcal{S}_3$  remain nevertheless quasi-degenerate). The energy of some of these states and the energy of the states of  $\mathcal{S}_3$  decrease with increasing  $J'$  and become comparable to the energy of the states  $|5\rangle$ ,  $|7\rangle$ ,  $|8\rangle$  for  $J' \sim 0.6$ . Yet, up to  $J' = 0.4$  the evolution vs  $1/L$  of the gaps  $\Delta_i^0$  to the states of  $\mathcal{S}_1$  and  $\mathcal{S}_2$  shows that these splitting are much reduced for  $L \rightarrow \infty$ . All the gaps to the states of  $\mathcal{S}_1$ ,  $\mathcal{S}_2$  and  $\mathcal{S}_3$  extrapolate to  $\approx 0$ . The singlet spectrum thus remains close to the one of independent chains. The finite-size results give nevertheless a first indication that the splitting of the states in  $\mathcal{S}_1$ ,  $\mathcal{S}_2$  will subsist for  $L \rightarrow \infty$ . A differentiation in the extrapolated values of the gaps becomes more visible at larger  $J'$  values.

Fig. 18 shows the evolution of the singlet-gaps  $\Delta_i^0$  vs  $1/L$  for the  $M = 4$  samples at  $J' = 0.8$  and  $J_2 = 0.45$ . The evolutions of the  $\Delta_i^0$  still remain quasi-linear with  $1/L$  if  $L \leq 8$  ( $N \leq 32$ ) on  $J_2^m(J')$  up to  $J' = 0.8$ . A curvature is hardly visible. But, since a linear extrapolation for  $N > 32$  would lead to negative values for  $\Delta_1^0$ ,  $\Delta_2^0$ ,  $\Delta_3^0$ ,  $\Delta_6^0$ , an upward curvature may be inferred for these gaps. This affects the precision of the extrapolations for  $L \rightarrow \infty$  but one may conjecture, in view of Fig. 18, that not only  $\Delta_2^0$  still likely vanishes as at  $J_2 = 0.4$ , but also  $\Delta_1^0$ , whereas the other  $\Delta_i^0$  are very small and some may vanishes. This could be the case of  $\Delta_3^0$ ,  $\Delta_6^0$  which extrapolate to negative values and probably  $\Delta_4^0$  which follow closely  $\Delta_3^0$  for all sizes if  $J' \leq 0.8$ . The vanishing of  $\Delta_6^0$  is nonetheless uncertain as the degeneracy of state  $|6\rangle$  with the state  $|2\rangle$  seems to be lifted on the line  $J_2^m(J')$ . But  $\Delta_7^0$ ,  $\Delta_8^0$  and probably  $\Delta_5^0$  which extrapolate above  $\Delta_4^0$  remain finite and thus the degeneracies which occur for decoupled chains are lifted. Nonetheless these gaps

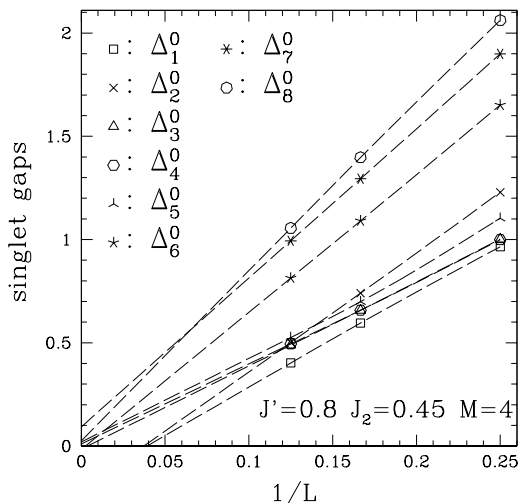


FIG. 18. Singlet-gaps  $\Delta_i^0$  (see text) at  $J' = 0.8$  and  $J_2 = 0.45$  vs  $1/L$  for for  $N = 16, 24, 32$  samples of  $M = 4$  chains. The dashed lines are spline fit to the data for  $N \leq 32$  followed by linear extrapolation for  $N > 32$ .

remain probably very small which suggest that they open exponentially like the spin-gap. The gaps to the states at the bottom of the singlet continuum are also small. Those to the states of  $\mathcal{S}_3$  extrapolate to quasi-vanishing values. The spectrum appears to be gapless or quasi-gapless.

The exact degree of ground-state degeneracy is difficult to ascertain, especially for  $M = 6$ . The most likely vanishing gaps are  $\Delta_1^0$ ,  $\Delta_2^0$ ,  $\Delta_3^0$ ,  $\Delta_4^0$ ,  $\Delta_6^0$  for  $M = 4$ . This would lead to a  $2^{M-1} = 8$  ground-state degeneracy. Yet the degeneracy would be limited to 6 if  $\Delta_6^0$  remains finite. Besides the gaps to the lowest states in the singlet continuum appear to be quasi-vanishing. For  $M = 6$ , the extrapolations of the singlet gaps, although even more unaccurate than for  $M = 4$ , also indicate a large ground-state degeneracy and a gapless continuum of singlet excitations adjacent to the ground-state. This also suggests a spectrum that correspond closer to the one of the RVB state of NT than to the one of independent chains.

This degeneracy of additional singlet states is accompanied with a modification of the pattern of the dimer-dimer correlations  $D(i, j; k, l)$  as shown for  $N = 32$  in Fig. 19. Dimer-dimer correlations  $D(1, 5; k, l)$  between a reference horizontal pair  $(1, 5)$  and a pair  $(k, l)$  on the same chain remain strong but have now become extremely small otherwise, much weaker than for  $J_2 = 0.4$ , as shown in Fig. 19(a). As shown in Fig. 19(b), this is also the case for dimer-dimer correlations  $D(1, 4; k, l)$  between a vertical dimer on a pair of chains and vertical dimer on a different pair of chains, whereas  $D(1, 4; k, l)$  remain of significant magnitude for pairs of dimers joining the same chains. Fig. 19(a)(b) give a picture of strongly correlated pairs of adjacent chains, decorrelated from one

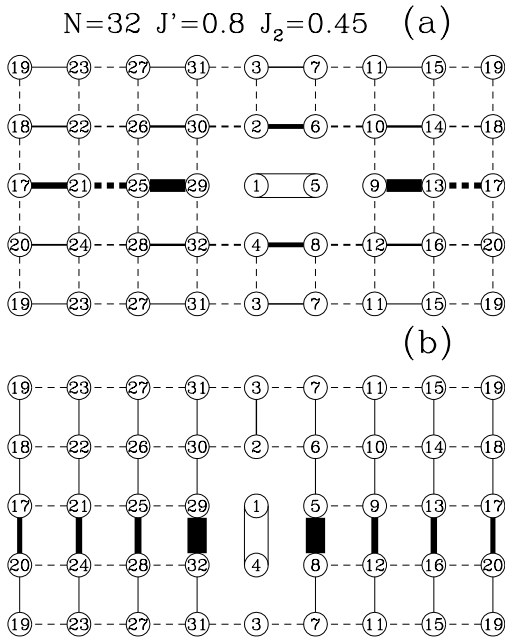


FIG. 19. Dimer-dimer correlation function (see Fig 16) for  $N = 32$ ,  $J' = 0.80$   $J_2 = 0.45$ .

pair to the next with dimer long range correlations along individual chains and along the rungs of pairs of adjacent chains. This pairing is reminiscent of the RVB state of NT.

The ED results thus indicate a behavior close to the one of independent chains on  $J_2^m(J')$  up to very large interchain coupling but which differs. Instead they suggest that the RVB behavior predicted by NT at weak interchain coupling may be realized and also extends at large interchain coupling, perhaps up to  $J' = 0.8$ , if  $J_2 \approx J_2^m(J')$ .

The extension of the RVB state on  $J_2^m(J')$  would however have an upper limit. For  $J' \gtrsim 0.9$  the evolution of the singlet gaps vs  $1/L$  show that they are clearly finite if  $L \rightarrow \infty$  for  $M = 4$ . This would imply a transition on  $J_2^m(J')$ . The transition might be discontinuous as the gaps seems to open abruptly. An alternative possibility could be that the RVB state is only approximately realized on  $J_2^m(J')$ . The degeneracy of the RVB state would be progressively lifted with increasing  $J'$  but slower than the degeneracy corresponding to the independent chain behavior.

The ED results on the  $M = L$  samples of  $N = 16, 36$  spins at  $J' = J$  indicate that the behavior of the  $J_1 - J_2$  model for  $J_2^m$  differs from the one at  $J' < J$ . But several features reminiscent of this state subsists. The lowest triplet excitations have only a small dispersion on the boundary of the Brillouin zone. The singlet spectrum at finite size is rather similar to the one for  $J' < J$ : one finds low lying states with wave vector on the side of the Brillouin zone in addition to  $|1\rangle$ ,  $|2\rangle$ ,  $|3\rangle$  (degenerate with  $|2\rangle$ ) which would allow to form a four-fold degenerate columnar VBC. The  $J_1 - J_2$  model for  $J_2^m$ , if it displays VBC order, is nonetheless close to a state with a spin-liquid behavior at this point of the phase diagram.

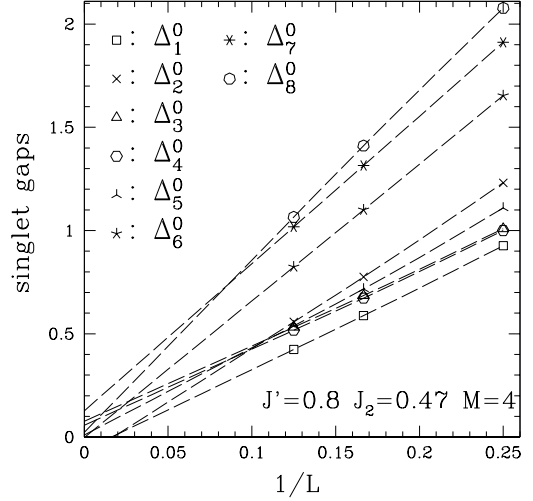


FIG. 20. Same as Fig. 18 at  $J' = 0.8$  and  $J_2 = 0.47$ .

### C. $J_2 > J_2^m$

The behavior predicted by NT is also most likely limited to the line  $J_2^m(J')$ . Increasing  $J_2$  at fixed  $J'$  one finds a narrow region with a different behavior before reaching the region where the spectra display the features of the  $(\pi, 0)$  Néel phase. The spin-spin correlations  $s(l, m)$  (Eq. 5.1) at  $J' \leq 0.8$  have now the same signs as in the  $(\pi, 0)$  Néel phase:  $s(l, m) \sim -1^l$ , alternating in sign in the horizontal direction and being ferromagnetic along vertical lines. Fig. 20 shows the evolution of the singlet gaps at  $J' = 0.8$ ,  $J_2 = 0.47$  for  $M = 4$  which indicate that singlet gaps have opened except  $\Delta_1^0$  and  $\Delta_2^0$  which may still vanish. This excludes an eight-fold degeneracy of the ground-state. But the exact degeneracy of the ground-state is difficult to ascertain. The region is very narrow (all singlet gaps are clearly finite at  $J_2 = 0.5$  when  $J' = 0.8$ ), much narrow than the region between the  $(\pi, \pi)$  Néel phase and the line  $J_2 = J_2^m(J')$ . Due to the proximity of the line  $J_2 = J_2^m(J')$  where  $\Delta_1^0$ ,  $\Delta_2^0$  would vanish it is difficult to conclude whether both  $\Delta_1^0$  and  $\Delta_2^0$  really vanishes.

The patterns of dimer-dimer correlations are shown in Fig. 21 for  $N = 32$  and  $M = 4$  at  $J' = 0.8$ ,  $J_2 = 0.47$ . The correlations between horizontal dimers in Fig. 21(a) display a similar alternation of sign as in Fig. 16(a) and could be compatible with a columnar  $(\pi, 0)$  VBC LRO, although they have a small magnitude if the bonds are on different chains.

As the shortest pair of spins with the next largest AF spin-spin correlations are on the diagonals of a square, whereas the vertical nearest neighbor spins are ferromagnetically correlated, we have displayed the correlations between diagonal bonds (Fig. 21(b)) and between diagonal and horizontal bonds (Fig. 21(c)).

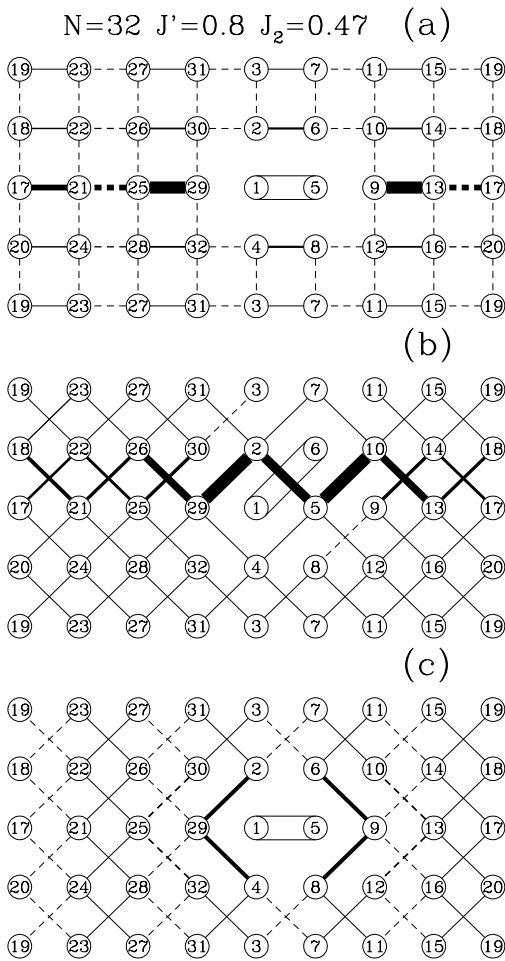


FIG. 21. Dimer-dimer correlation functions (see Fig 16) for  $N = 32$ ,  $J' = 0.80$   $J_2 = 0.47$ .

As shown in Fig. 21(b), the correlations between diagonal bonds  $D(1, 6; k, l)$  do not show a clear modulation in their magnitudes neither in the horizontal, the vertical or the diagonals directions.  $D(1, 6; k, l)$  is small except for bonds linking two adjacent chains. There subsists a tendency of pairs of adjacent chains to associate as seen in Fig. 19(b). The correlations are then rather similar to those in the 'Haldane phase' of the two-leg ladder. There is no visible tendency of the diagonal bonds to order.

As shown in Fig. 21(c), the correlations between a horizontal bond and a diagonal bond in the same column are negative and there is a sign alternation of the correlations between an horizontal bond and diagonal bonds in the horizontal direction similar to alternation in Fig. 21(a), compatible with a breaking of translational symmetry in the horizontal direction.

A vanishing of  $\Delta_1^0$ ,  $\Delta_2^0$  would lead to a three-fold ground-state degeneracy, but the pattern of dimer-dimer correlations do not indicate a VBC LRO with a three-fold degeneracy of states  $|0\rangle$ ,  $|1\rangle$ ,  $|2\rangle$ .

On the other hand, a columnar VBC LRO with plaquette modulation, which would lead to an additional translational symmetry breaking in the vertical direction, appears also unlikely for  $J' \leq 0.8$  in view of the pattern of dimer-dimer correlations and the fact that the gap  $\Delta_3^0$

to the singlet state  $|3\rangle$  with wave-vector  $(0, \pi)$  is finite.

If there is VBC LRO, it is most probably a  $(\pi, 0)$  like VBC LRO. It will be associated with a vanishing of  $\Delta_2^0$  whereas  $\Delta_1^0$  will be finite. The small but noticable upward curvature in the evolution of  $\Delta_1^0$  in Fig. 20 supports indeed that  $\Delta_1^0$  might be finite for  $L \rightarrow \infty$  in this region for  $J' = 0.8$ .

As for  $J_2 < J_2^m$ , the  $(\pi, 0)$  VBC LRO disappears for  $J' < 1$  if  $M$  is finite but could extend for  $J' \rightarrow 1$  if  $M = L \rightarrow \infty$ . A  $(\pi, 0)$  LRO would mean that there is the same kind of VBC LRO on both sides of  $J_2^m(J')$  for  $M \geq 4$ . The state for  $J_2^m(J') \lesssim J_2$  could however differs from the state for  $J_2 \lesssim J_2^m(J')$  by some non-local order parameter similar to those of the 'singlet state' and the 'Haldane state' of the two-leg ladder as conjectured at the end of Sec. IV for the phases at finite  $M > 2$  on both sides of the intermediate region.

## VI. SUMMARY

Exact diagonalization calculations provide support that the RVB behavior predicted by Nersesyan and Tsvelik in the  $J - J' - J_2$  model at  $J_2 = 0.5J' \ll J$  may be realized and extends along a curve coincident with the line of maximum frustration  $J_2^m(J')$  where it subsists up to large interchain coupling for an even number  $M$  of chains of length  $L \rightarrow \infty$ . The line  $J_2^m(J')$  is the analogue of the transition line  $J_2 = 0.5J'$  in the classical model on which the chains decouples. The independent chain behavior appears destabilized by quantum fluctuations.

The line  $J_2^m(J')$  is located in an intermediate region of the phase diagram where the present results suggest that the ground-state displays a columnar  $(\pi, 0)$  valence bond long range order. This region of columnar order will have a finite width as soon as  $M \leq 4$  and extends on both sides of  $J_2^m(J')$  up to a value of  $J'$  close but smaller than  $J$  for finite  $M$ , that increase with  $M$  and approach  $J' = J$  for  $M = L \rightarrow \infty$ . It separates two phases that are fully gapped Haldane like phases for finite  $M$  and evolves respectively to the  $(\pi, \pi)$  and  $(\pi, 0)$  Néel phases for  $M \rightarrow \infty$ . The Haldane like phases have probably a topological order. Its nature for  $M > 2$  deserves further investigation.

The occurrence of a columnar order for  $J'$  smaller than  $J$ , next to the Néel phase, agrees with the scenario deduced from large- $N$  approaches that valence bond crystal order is expected after the destabilization of a collinear AF Néel phase. It is possible that the columnar order may extend for  $J' \rightarrow J$  if  $M = L \rightarrow \infty$  and that this scenario may be realized also in the  $J_1 - J_2$  model which corresponds to  $J' = J$ . The behavior of the  $J - J' - J_2$  model in the intermediate region for  $J' \rightarrow J$  requires nonetheless further study to confirm this hypothesis.

Acknowledgments: I thank Patrick Azarian, Philippe Lecheminant and Claire Lhuillier for fruitful discussions. Computations were performed at The Centre de Calcul

pour la Recherche de l'Université Pierre et Marie Curie and at the Institut de développement des Recherches en Informatique Scientifique du CNRS under contract 990076.

- 
- [1] N. Read and S. Sachdev, Phys. Rev. B **42**, 4568 (1990).  
[2] N. Read and S. Sachdev, Phys. Rev. Lett. **66**, 1773 (1991).  
[3] S. Sachdev and K. Park, Annals of Physics (N.Y.) **298**, 58 (2002).  
[4] J.-B. Fouet, P. Sindzingre, and C. Lhuillier, Eur. Phys. J. B **20**, 241 (2001).  
[5] P. Sindzingre, J.-B. Fouet, and C. Lhuillier, Phys. Rev. B **66**, 174424 (2002).  
[6] J.-B. Fouet, M. Mambrini, P. Sindzingre, and C. Lhuillier, Phys. Rev. B **67**, 054411 (2003).  
[7] A. Läuchli, S. Wessel and M. Sigrist, Phys. Rev. B **66**, 014401 (2002).  
[8] H. Schulz and T. A. L. Ziman, Eur. Phys. Lett. **18**, 355 (1992).  
[9] H. Schulz, T. A. L. Ziman and D. Poilblanc, J. Phys. I (France) **6**, 675 (1996).  
[10] R. R. P. Singh, Z. Weihong, C. J. Hamer, and J. Oitmaa, Phys. Rev. B **60**, 7278 (1999).  
[11] V. N. Kotov, Jaan Oitmaa, Oleg Sushkov, Zheng Weihong, Phil. Mag. B **80**, 1483 (2000).  
[12] L. Capriotti and S. Sorella Phys. Rev. Lett. **84**, 3173 (2000).  
[13] M. S. L. du Croo de Jongh, J. M. J. van Leeuwen, W. van Saarloos Phys. Rev. B **62**, 14844 (2000).  
[14] O. P. Sushkov, J. Oitmaa, and Z. Weihong, Phys. Rev. B **63**, 104420 (2001).  
[15] L. Capriotti, F. Becca, A. Parola and S. Sorella, Phys. Rev. Lett. **87**, 097201 (2001).  
[16] O. P. Sushkov, J. Oitmaa, and Zheng Weihong, Phys. Rev. B **66**, 054401 (2002).  
[17] L. Capriotti, F. Becca, A. Parola and S. Sorella, Phys. Rev. B **67**, 212402 (2003).  
[18] A. A. Nersesyan and A. M. Tsvelik Phys. Rev. B **67**, 024422 (2003).  
[19] F. A. Smirnov and A. M. Tsvelik, cond-mat/0304634  
[20] M. J. Bhaseen and A. M. Tsvelik, cond-mat/0305194  
[21] Zheng Weihong, V. Kotov and J. Oitmaa Phys. Rev. B **57**, 11439 (1998).  
[22] Xiaoqun Wang, condmat/9803290 (unpublished); Mod. Phys. Lett. B **14**, 32 (2000)  
[23] T. Hakobyan, J. H. Hetherington, and M. Roger Phys. Rev. B **63**, 144433 (2001)  
[24] Dave Allen, F. H. L. Essler and A. A. Nersesyan, Phys. Rev. B **61**, 8871 (2000).  
[25] Xiaoqun Wang, N. Zhu and C. Chen Phys. Rev. B **66**, 172405 (2002).  
[26] F. D. M. Haldane, Phys. Lett. **93A**, 464 (1983)  
[27] S. R. White, R. M. Noack, and D. J. Scalapino Phys. Rev. Lett. **73**, 886-889 (1994).  
[28] M. Greven, R. J. Birgeneau, U.-J. Wiese Phys. Rev. Lett. **77**, 1865 (1996).  
[29] B. Frischmuth, B. Ammon, and M. Troyer Phys. Rev. B **54**, R3714 (1996).  
[30] A. W. Sandvik, Phys. Rev. Lett. **83**, 3069 (1999).  
[31] P. Hasenfratz and F. Niedermayer, Z. Phys. B. Condensed Matter **92**, 91 (1993).  
[32] S. R. White, Phys. Rev. B **53**, 52 (1996).  
[33] P. Azaria, P. Lecheminant and A. A. Nersesyan Phys. Rev. B **58**, R8881 (1998)  
[34] S. Moukouri, cond-mat/0305608 (unpublished).  
[35] B. Bernu, C. Lhuillier, and L. Pierre, Phys. Rev. Lett. **69**, 2590 (1992)  
[36] Shaojin Qin, Jizhong Lou, Liqun Sun and Changfeng Chen, Phys. Rev. Lett. **90**, 067202 (2003).  
[37] P. Sindzingre, G. Misguich, C. Lhuillier, B. Bernu, L. Pierre, Ch. Waldtmann, and H.-U. Everts Phys. Rev. Lett. **84**, 2953-2956 (2000).